

Composite search of active particles in three-dimensional space based on non-directional cues

Justus A. Kromer,¹ Andrea Auconi,² and Benjamin M. Friedrich^{2,*}

¹Stanford University, Stanford, California, United States of America

²TU Dresden, Dresden, Germany

(Dated: March 22, 2021)

We theoretically address minimal search strategies of active, self-propelled particles towards hidden targets in three-dimensional space. The particles can sense if a target is close, e.g., by detecting signaling molecules released by a target, but they cannot deduce any directional cues. We focus on composite search strategies, where particles switch between extensive outer search and intensive inner search; inner search is started when the proximity of a target is detected and ends again when a certain inner search time has elapsed. In the simplest strategy, active particles move ballistically during outer search, and transiently reduce their directional persistence during inner search. In a second, adaptive strategy, particles exploit a dynamic scattering effect by reducing directional persistence only outside a well-defined target zone. These two search strategies require only minimal information processing capabilities and a single binary or tertiary internal state, respectively, yet increases the rate of target encounter substantially. The optimal inner search time scales as a power-law with exponent $-2/3$ with target density, reflecting a trade-off between exploration and exploitation.

Keywords: active Brownian particle, intermittent search, non-directional cues, chemokinesis, persistent random walk, correlated random walk

Turning active colloids into micro-scale robots will enable envisioned biomedical or environmental applications [1, 2]. Yet, the information processing capabilities of these self-propelled agents remain limited. This motivates theoretical analysis of minimal strategies that are simultaneously simple and effective. Here, we address optimal random search for hidden targets [3, 4]. We propose a minimal model of an Active Brownian Particle (ABP) that regulates its directional persistence in response to local cues. Previous work showed that for ABP without internal states or memory, such a chemokinesis strategy does not provide any advantage compared to simple ballistic motion [5]. Yet, a single binary or tertiary internal state allows these agents to increase their rate of target encounter substantially.

Our question is thus: *How to continue a random search for hidden targets if information is received that a target must be close, yet no directional information is given?* This situation frequently arises when search agents detect dilute chemical signals released by targets. Examples include chemokinetic navigation of motile cells, foraging of animals [6], and odor-sniffing robots [7, 8]. For micrometer-sized agents, the signal-to-noise ratio of sensing chemical gradients is low at sub-nanomolar concentrations, preventing effective directed chemotaxis, notwithstanding the fact that the chemical signal itself is above detection threshold, and thus indicates the proximity of a target releasing signaling molecules.

If search agents can only detect the presence of a nearby target within a given threshold distance, we can decompose the search problem into an *outer* and an *inner* search problem, far and close to a target, respectively. While the main purpose of outer search is the *ex-*

ploration of search space (extensive search [9]), the agent may choose a different *exploitation* strategy in the vicinity of a target for inner search (intensive search). Composite search strategies allow agents to switch between different search modes [9–15], e.g., for outer and inner search.

The performance of search strategies strongly depends on the dimension of search space. According to Pólya’s theorem [16], a diffusive particle will eventually find a target in one- and two-dimensional space almost surely, while such a particle may never find the target in three dimensional space. A colloquial version of Pólya’s theorem states: *A drunk man will find his way home, but a drunk bird may get lost forever* [17]. This marks an important qualitative difference between search problems in two and three space dimensions. Previous research often investigated search problems in two-dimensional space, largely motivated by animal foraging. Among others, this includes theoretical and computational studies of composite search strategies for hidden targets [14, 18–21], the narrow escape problem [21–24], or local search around a home base [25, 26]. Yet, microswimmers must usually search a three-dimensional environment. Therefore, in the present manuscript, we focus on the less-studied problem of search in three-dimensional space.

The optimal strategy for outer search depends on the distribution of target sites: while Lévy walks are optimal for certain fractal distributions of targets (or if targets can be revisited), simple ballistic motion is optimal in infinite domains with uncorrelated random target positions, where each target can be visited only once [27–29]. This latter case exactly corresponds to a well-stirred suspension of targets (which are consumed upon encounter),

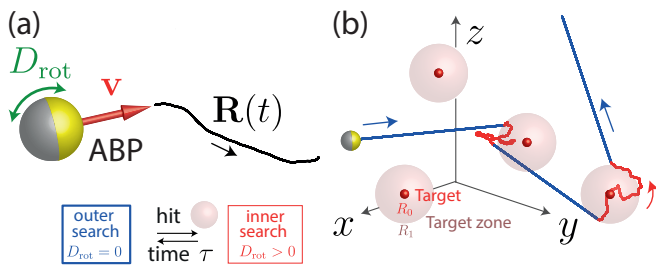


FIG. 1: **Composite search.** (a) We consider an Active Brownian Particle (ABP) with velocity v and rotational diffusion coefficient D_{rot} as a generic model of a self-propelled microswimmer. (b) The ABP searches for randomly distributed hidden targets (red) in three-dimensional space, alternating between an *outer search* (blue, here corresponding to ballistic motion), and *inner search* for a restricted time τ , (red, here corresponding to low-persistence motion). Inner search is triggered whenever the ABP senses the vicinity of a target (rosé), and ends once a certain inner search time τ has elapsed. This defines a composite search strategy based on non-directional cues.

and we will therefore assume ballistic motion for outer search.

Directional persistence is a key kinetic parameter of self-propelled microswimmers, which is set by a competition between swimming speed and directional fluctuations; directional fluctuations can be of thermal origin or originate from active fluctuations of the propulsion mechanism itself. A microswimmer may thus *control* its directional persistence by different means: (i) transiently changing its speed [30], for instance in response to the local concentration of a chemical [31] or external fields [32], (ii) transiently changing its effective size L (since the thermal rotational diffusion coefficient changes as $\sim 1/L^3$ [33]), or (iii) up- or down-regulating any stochastic part of active propulsion [34, 35]. Despite these different possible implementations, we will consider a generic model, assuming agents can effectively regulate their directional persistence.

In this short communication, we consider a minimal model of an active particle that employs composite search in three-dimensional space. The particle switches between ballistic motion in outer search and intensive inner search. Our model generalizes Active Brownian Particles (ABP), frequently used as minimal model for cell motility, e.g. of biological or artificial microswimmers [36, 37] (also called correlated or persistent random walkers [38–40]). We find that a single binary internal state allows these agents to substantially increase their rate of target encounter. The optimal inner search time (‘giving-up time’) decreases with target density ρ as $\sim \rho^{-2/3}$, reflecting an exploration-exploitation trade-off [41] between continuing inner search to eventually find the nearest target, or searching elsewhere for other targets.

Model: Active Brownian Particles. We consider an ABP moving along a trajectory $\mathbf{R}(t)$ in three-dimensional space with speed v and rotational diffusion coefficient D_{rot} . Rotational diffusion causes its tangent $\mathbf{t} = \dot{\mathbf{R}}/v$ to decorrelate on a time-scale $\tau_p = l_p/v$ set by the persistence length $l_p = v/(2D_{\text{rot}})$, i.e., $\langle \mathbf{t}(t_0) \cdot \mathbf{t}(t_0 + t) \rangle = \exp(-|t|/\tau_p)$ [42].

We first consider the case of a single spherical target of radius R_0 located at $\mathbf{R}=\mathbf{0}$. Due to spherical symmetry, the time-dependent distance $R(t) = |\mathbf{R}(t)|$ of the agent to the origin, and the time-dependent angle $\psi(t)$ enclosed by the tangent \mathbf{t} and the radial direction $\mathbf{e}_R = -\mathbf{R}/R$, decouple from other coordinates [5, 43, 44]

$$\dot{R} = -v \cos \psi, \quad (1)$$

$$\dot{\psi} = \frac{v}{R} \sin \psi + \sqrt{2D_{\text{rot}}} \xi(t) + D_{\text{rot}} \cot \psi. \quad (2)$$

Here, $\xi(t)$ is Gaussian white noise with $\langle \xi(t) \rangle = 0$ and $\langle \xi(t)\xi(t') \rangle = \delta(t-t')$.

Intriguingly, the case of a position-dependent speed $v(\mathbf{x})$ (*orthokinesis* [6]), and the case of a position-dependent rotational diffusion coefficient $D_{\text{rot}}(\mathbf{x})$ (*klinokinesis*) can be mapped onto each other using a local re-parameterization of time [5]: if we formally re-scale local time by a factor $\Phi = v_0/v(\mathbf{x})$, then ABPs apparently move with constant speed $v_0 = v(\mathbf{x})\Phi$, while the new rotational diffusion coefficient reads $D_{\text{rot}}\Phi$. We emphasize that the shapes of trajectories do not change under such time re-parametrization. For ABP with constant speed, it is known that the steady-state probability distribution $p^*(\mathbf{x})$ is spatially homogeneous, even if the rotational diffusion coefficient $D_{\text{rot}}(\mathbf{x})$ depends on position [5, 45, 46].

In the following, we assume a minimal model with constant speed v and switchable rotational diffusion coefficient D_{rot} , as detailed next.

Inner and outer search. We now turn to the full search problem for multiple, non-revisitable targets (Poisson distributed with density ρ), combining inner and outer search, see Fig. 1. In outer search mode, the ABP moves ballistically ($D_{\text{rot}} = 0$), i.e., it uses the optimal strategy to find non-revisitable targets [27–29]. Close to a target, the ABP uses time-restricted inner search with high rotational diffusion coefficient D_{rot} (low directional persistence), see Fig. 1. This simple strategy only requires the agent to detect that a target must be within a detection radius R_1 .

Whenever the ABP enters one of the spheres of radius R_1 surrounding the targets, it switches to one of the following *inner search* strategies for a limited inner search time τ :

(i-a) *Inner search with fixed inner search time:* The ABP transiently increases its rotational diffusion coefficient D_{rot} (i.e., reduces its directional persistence) upon detecting a target zone for a total duration τ (red curves in Fig. 2).

(i-b) *Stochastic timer*: Same as strategy (i-a), but for random inner search times τ drawn from a distribution $q(\tau)$ with mean $\bar{\tau}$ (blue curves in Fig. 2).

(ii) *Adaptive inner search*: During inner search, the ABP uses a position-dependent rotational diffusion coefficient $D_{\text{rot}}(\mathbf{x})$ that depends on its distance R from the nearest target: the agent uses ballistic motion with $D_{\text{rot}} = D_1 = 0$ if the target is within the detection radius with $R \leq R_1$, while the agent moves with reduced directional persistence with $D_{\text{rot}} = D_2 > 0$ for $R > R_1$. This strategy exploits a generic scattering effect that provides ABPs with multiple search attempts [5]. Like in strategy (i-a), inner search is terminated after an inner search time τ , after which the agent resumes outer search with only ballistic motion until proximity of the next target is detected. Below we show that the rate of target encounter is increased for adaptive inner search (black curves in Fig. 2).

(i-a) *Fixed inner search time*. We introduce a strict *timer* for inner search: The ABP automatically resets its internal state back to outer search after a maximal inner search time τ (except in the unlikely event that the agent finds itself again in a target zone defined by $R \leq R_1$). This defines a *composite search* strategy [14].

What is the optimal time τ_{opt} the ABP should spend in ‘inner search mode’ before switching back to ballistic motion (‘giving-up time’ [14]), in order to maximize the rate k of target encounters? The answer depends on the density of targets ρ and the probability $p_{\text{in}}(\tau)$ of successful inner search within time τ . The derivative $\mathcal{F}(\tau) = dp_{\text{in}}(\tau)/d\tau$ denotes the (non-normalized) distribution of first-passage times for inner search.

For composite search consisting of inner and outer search, we have $k = k_{\text{out}} p_{\text{in}}(\tau)$, where k_{out} denotes the rate at which the ABP enters the target zone around some target. For ballistic motion, k_{out} equals the product of ρ and the effective search volume per unit time $\sigma = \pi R_1^2 v$ [47]. Thus, $k_{\text{out}} \approx \rho \sigma (1 - k_{\text{out}} \tau)$, where we take into account the time fraction $k_{\text{out}} \tau$ spent in inner search. We neglect the small probability that the ABP is again inside a target zone at the end of inner search. This expression can be rewritten as $k_{\text{out}} = [(\rho \sigma)^{-1} + \tau]^{-1}$. The optimal duration τ_{opt} of inner search that maximizes $k(\tau)$ must satisfy $0 = \partial k / \partial \tau|_{\tau=\tau_{\text{opt}}}$, which we can re-arrange as

$$\frac{\partial}{\partial \tau} \ln p_{\text{in}}(\tau)|_{\tau=\tau_{\text{opt}}} = [(\rho \pi R_1^2 v)^{-1} + \tau_{\text{opt}}]^{-1} . \quad (3)$$

Eq. (3) embodies the trade-off between continuation of inner search and decampment to new targets in the spirit of a *Marginal Value Theorem* [48]. If targets are denser, less time should be spent in inner search, see Fig. 2(b), red curves. For long times $\tau D_{\text{rot}} \gg 1$, persistent random walks can be approximated by diffusion. This implies

an asymptotic Sparre-Anderson scaling $dp_{\text{in}}/d\tau \sim \tau^{-3/2}$ [49]. In the limit of sparse targets, where the volume fraction occupied by the target zones of all targets is much smaller than one, $\rho V_1 \ll 1$, a straight-forward but lengthy calculation gives (see Supplemental Material (SM) text)

$$\tau_{\text{opt}} \sim \rho^{-2/3} . \quad (4)$$

The ABP will spend considerably more time in outer search compared to inner search, $k_{\text{out}} \tau_{\text{opt}} \ll 1$. Together with $p_{\text{in}}(\tau_{\text{opt}}) \lesssim \lim_{\tau \rightarrow \infty} p_{\text{in}}(\tau) \approx R_0/R_1$, we conclude for the rate of target encounter for composite search, $k \approx \rho \pi R_0 R_1 v$. We may re-state this result equivalently as follows: composite search with fixed inner search time according to strategy (i-a) increases the effective cross-sectional area of target encounter to $k/(\rho v) \lesssim \pi R_0 R_1$, compared to $k/(\rho v) = \pi R_0^2$ for pure ballistic motion. A detailed mathematical derivation can be found in SM text.

(i-b) *Stochastic timer*. Above we considered the case of a fixed inner search time τ for sake of simplicity, yet real artificial microswimmers will likely not be able to control inner search time precisely. Instead, we expect that the microswimmer can only realize a distribution $q(\tau)$ of inner search times that vary around a mean value $\bar{\tau}$. In the possibly simplest example, switching back to outer search mode could be controlled by a single-rate process with rate constant $1/\bar{\tau}$; in this case, inner search times τ follow an exponential distribution with mean $\bar{\tau}$

$$q_{\bar{\tau}}(\tau) = \bar{\tau}^{-1} \exp(-\tau/\bar{\tau}) . \quad (5)$$

All results derived above hold also in this case (and in fact even for $q_{\bar{\tau}}(\tau) = \bar{\tau}^{-1} f(\tau/\bar{\tau})$ with some arbitrary function f), provided the probability $p_{\text{in}}(\tau)$ of successful inner search is replaced by an effective probability distribution $\bar{p}_{\text{in}}(\bar{\tau}) = \int_0^\infty d\tau p_{\text{in}}(\tau) q_{\bar{\tau}}(\tau)$. In particular, we have the asymptotic scaling $d\bar{p}_{\text{in}}/d\bar{\tau} \sim \bar{\tau}^{-3/2}$, and Eq. (4) holds analogously for the optimal mean inner search time $\bar{\tau}$, see Fig. 2, blue curves.

(ii) *Adaptive inner search*. The probability for successful inner search $p_{\text{in}}(\tau)$ can be further increased by choosing an even more efficient inner search strategy [5]. Instead of using a constant rotational diffusion coefficient D_{rot} during inner search, the agent may employ a position-dependent rotational diffusion coefficient $D_{\text{rot}}(\mathbf{x})$ during inner search and switch its rotational diffusion coefficient between two values D_1 and D_2 inside and outside a target zone of radius R_1 around the target, respectively. If $D_1 \ll D_2$, this adaptive inner search strategy increases the probability to eventually find the target substantially by exploiting a dynamic scattering effect [5]. In short, ABP that head away from the target will switch to motion with low directional persistence as soon as they move beyond distance R_1 , which results in a high probability to reverse direction and enter the target

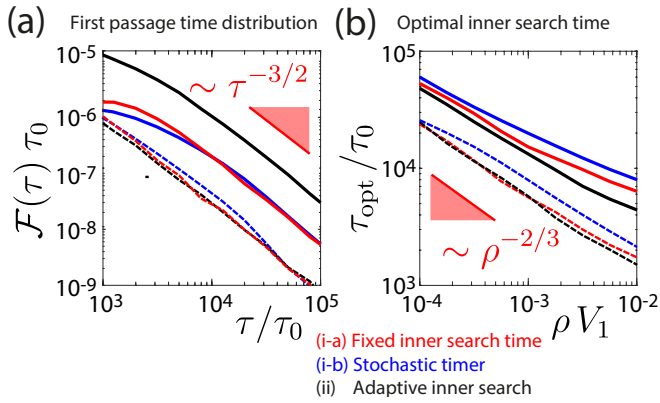


FIG. 2: **Optimal inner search time decreases with target density.** (a): Simulated probability density $\mathcal{F}(\tau) = dp_{\text{in}}(\tau)/d\tau$ of first-passage times τ to find a spherical target of radius R_0 for search agents starting at a distance R_1 from the target for different variants of inner search. Red curves: agents with constant rotational diffusion coefficient D_{rot} in inner search [strategy (i-a)]. Black: agents employing adaptive inner search [strategy (ii)] with ballistic motion inside the target zone $R \leq R_1$ and constant rotational diffusion coefficient D_{rot} outside, as in [5]. Blue curves: probability density $\bar{\mathcal{F}}(\bar{\tau}) = d\bar{p}_{\text{in}}(\bar{\tau})/d\bar{\tau}$ to find the target for agents with stochastic timer, for which maximal inner search time follows an exponential distribution with mean $\bar{\tau}$, see Eq. (5) [strategy (i-b)]. All curves: dashed: $D_{\text{rot}}=v/(4R_0)$, solid: $D_{\text{rot}}=10v/(4R_0)$, time-scale $\tau_0 = R_0/v$. The probability densities are not normalized, as the total probability to eventually find the target is less than one even for infinite search times. (b): Optimal time limit τ_{opt} for inner search decreases for increasing target density [cases as in panel (a)]. Parameters: $R_1/R_0 = 20$, volume of target zone $V_1=4\pi R_1^3/3$.

zone again. There, the ABP resumes ballistic motion, providing the ABP with another attempt to hit the target. In the following, we set $D_1 = 0$ for the rotational diffusion coefficient D_{rot} inside the target zone.

An analytical calculation shows that the normalized rate of target encounter, $k/(v\rho)$, which represents an effective cross-sectional area of targets, equals πR_1^2 for adaptive search in the limit of sparse targets ($\rho V_1 \ll 1$) and large rotational diffusion coefficient ($D_2 \gg v/R_0$), see SM text for details. For comparison, we had found lower effective cross-sectional areas $k/(v\rho) \lesssim \pi R_0 R_1$ for inner search with constant $D_{\text{rot}} \gg v/R_0$, and $k/(v\rho) = \pi R_0^2$ for pure ballistic motion above, see also Fig. 3.

Numerical results confirm scaling law. Fig. 2(a) shows simulation results for the first passage time density $\mathcal{F}(\tau)$ to find the target exactly after time τ if the ABP starts at distance R_1 (with random initial direction as in [5]). For moderate values of the rotational diffusion coefficient D_{rot} , all three inner search strategies introduced above, i.e., inner search with *fixed timer* (red curves), inner search with *stochastic timer* (blue curves), and adaptive inner search (black curves), give rise to similar distributions $\mathcal{F}(\tau)$. For a high rotational diffusion co-

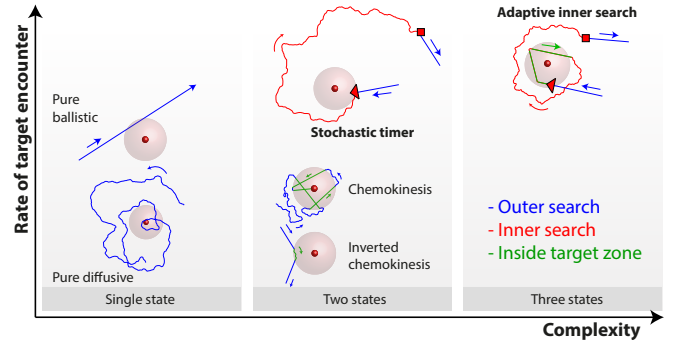


FIG. 3: **Comparison of random search strategies.** Shown are schematics of the different search strategies. In addition to the two strategies studied in this manuscript, composite search with *timer* for inner search, and *adaptive* inner search studied in this manuscript, *pure ballistic motion* (with $D_{\text{rot}} = 0$) and *pure diffusive motion* (with $D_{\text{rot}} \gg v/R_0$), as well as instantaneous *chemokinesis*, and *inverted chemokinesis* are shown. For instantaneous chemokinesis, the ABP changes its rotational diffusion coefficient instantaneously as function of target distance, with $D_{\text{rot}} = D_1$ inside the target zone (rosé, target distance $R \leq R_1$, green trajectory), and $D_{\text{rot}} = D_2$ outside the target zone ($R > R_1$, blue trajectory). The case $D_1 = 0$ and $D_2 \gg v/R_0$ labeled *chemokinesis* exploits a beneficial inward scattering effect, whereas the case $D_1 \gg v/R_0$ and $D_2 = 0$ labeled *inverted chemokinesis* suffers from disadvantageous outward scattering [5]. The different strategies are positioned according to a qualitative assessment of their control complexity and search performance. SM text contains quantitative results for the limit of low target density and high rotational diffusion coefficient.

efficient, however, the distribution $\mathcal{F}(\tau)$ is substantially higher for adaptive inner search. In all cases, numerical results confirm the asymptotic scaling $\mathcal{F}(\tau) \sim \tau^{-3/2}$.

Fig. 2(b) displays the corresponding optimal inner search time τ_{opt} , which was numerically determined from Eq. (3). Generally, strategies for which the density of first passage times is comparably higher for short inner search times τ display shorter optimal inner search times τ_{opt} . Intuitively, several short inner search episodes are more efficient than fewer longer ones. All cases confirm the asymptotic scaling $\tau_{\text{opt}} \sim \rho^{-2/3}$.

Discussion. We studied optimal search strategies for hidden targets, whose presence can be sensed at a distance. Using a minimal model of a chemokinetic agent that can switch between different rotational diffusion coefficients, we explain how search agents employing composite search find targets more efficiently if they possess memory in the form of an internal state (‘outer search mode’ versus ‘inner search mode’).

Intuitively, the improved search success can be explained as follows: if targets are randomly distributed in an infinite search domain (and can only be visited once), the optimal search strategy that maximizes the rate of target encounter is ballistic motion, i.e., moving simply along a straight path [27–29]. If a search

agent, however, receives the information that a target must be close, it is advantageous to transiently switch to less persistent motion to search the local neighborhood more thoroughly. Specifically, if a target of radius R_0 is known to be at most a distance R_1 away, the probability to eventually find this target using Brownian motion is $p^*(R_0|R_1) = R_0/R_1$ if search time is unlimited [50]. Mathematically, the conditional mean-first passage time to find the target diverges in this case, but this is not a practical limitation for search agents that use a finite inner search time. Indeed, a small fraction of eventually successful realizations will require a long time to reach the target (power-law tail of the distribution of conditional first-passage times). Yet, most of those realizations that reach the target will have done so already within a time-scale $\sim R_1^2/D_{\text{eff}}$, where $D_{\text{eff}} = v_0^2/(6D_{\text{rot}})$ is the effective translational diffusion coefficient of the search agent. Thus, the search agent faces a trade-off choice: shall it continue the inner search for a particular target that is known to have been close, to get closer to the best achievable probability $\lim_{\tau \rightarrow \infty} p_{\text{in}}(\tau)$ to find this particular target? Or rather give up inner search, wander off for good, and try to find other targets, to ultimately maximize its rate k of target encounters? This trade-off choice defines an optimal time τ_{opt} for inner search as function of target density: if the density ρ of targets is higher, it pays off to abandon inner search earlier, $\tau_{\text{opt}} \sim \rho^{-2/3}$.

Our generic framework allows to investigate different combinations of outer and inner search strategies, see also Fig. 3 and the SM. In general, strategies with ballistic motion during outer search outperform strategies with effective diffusive motion. For ballistic outer search, different inner search strategies differ in search performance (quantified in terms of an effective cross-sectional area of targets in the SM), with adaptive inner search performing best. Future work will address the effect of measurement noise in target zone detection. More complex strategies can be realized if agents respond in a gradual manner to the distance from the nearest target, e.g., in the form of distance-dependent swimming speed [30], distance-dependent rotational diffusion coefficient [5], or for dimers of elastically coupled active and passive particles in a spatial activity field [51].

Search strategies, such as the adaptive inner search strategy presented here, where agents increase their directional persistence when they move towards the target, are conceptually related to the principle of run-and-tumble chemotaxis, where changes in a temporal concentration signal regulate the strength of directional fluctuations [34]. Yet our minimal implementation is much simpler: in contrast to chemotaxis, it suffices if the agent compares local concentration of signaling molecules diffusing from a target to a fixed threshold.

Chemotactic navigation could additionally increase the probability to find the target when the search agent is already very close to the target and chemical gradients can

be measured with sufficient precision [52–56]. We speculate that composite random search as described here might have been an evolutionary precursor of chemotaxis strategies that additionally require sensory adaptation. Composite random search strategies without sensory adaptation may represent a promising route for the design of future active microswimmers that need to find hidden targets.

AA acknowledges support by the DFG (FR3429/3-1); BMF acknowledges support through the Heisenberg program of the DFG (FR3429/4-1); JAK, AA, and BMF were supported through the Excellence Initiative by the German Federal and State Governments (Clusters of Excellence cfaed EXC-1056 and PoL EXC-2068).

We would like to dedicate this manuscript to the memory of Lutz Schimansky-Geier.

-
- * Electronic address: benjamin.m.friedrich@tu-dresden.de
- [1] J. Li, B. E.-F. de Ávila, W. Gao, L. Zhang, and J. Wang, *Sci. Robot.* **2** (2017).
 - [2] B. Jurado-Sánchez and J. Wang, *Environ. Sci.: Nano* **5**, 1530 (2018).
 - [3] M. Mijalkov, A. McDaniel, J. Wehr, and G. Volpe, *Phys. Rev. X* **6**, 011008 (2016).
 - [4] L. G. Nava, R. Großmann, and F. Peruani, *Phys. Rev. E* **97**, 042604 (2018).
 - [5] J. A. Kromer, N. de la Cruz, and B. M. Friedrich, *Phys. Rev. Lett.* **124**, 118101 (2020).
 - [6] G. Fraenkel and D. Gunn, *The Orientation of Animals* (Dover Publ., New York, 1961).
 - [7] B. Webb, *Nature* **417**, 359 (2002).
 - [8] G. S. Settles, *J. Fluids Engin.* **127**, 189 (2005).
 - [9] S. Benhamou, *Ecol. Lett.* **17**, 261 (2014).
 - [10] S. Benhamou, *J. Theoret. Biol.* **159**, 67 (1992).
 - [11] M. J. Plank and A. James, *J. Roy. Soc. Int.* **5**, 1077 (2008).
 - [12] O. Bénichou, C. Loverdo, M. Moreau, and R. Voituriez, *Rev. Mod. Phys.* **83**, 81 (2011).
 - [13] F. Bartumeus, E. P. Raposo, G. M. Viswanathan, and M. G. da Luz, *PLOS One* **9**, e106373 (2014).
 - [14] B. C. Nolting, T. M. Hinkelman, C. E. Brassil, and B. Tenhumberg, *Ecol. Complex.* **22**, 126 (2015).
 - [15] V. V. Palyulin, A. V. Chechkin, R. Klages, and R. Metzler, *J. Phys. A* **49**, 394002 (2016).
 - [16] G. Pólya, *Math. Ann.* **84**, 149 (1921).
 - [17] Attributed to Shizuo Kakutani.
 - [18] P. Knoppien and J. Reddingius, *J. Theor. Biol.* **114**, 273 (1985).
 - [19] S. Benhamou, *Ecology* **88**, 1962 (2007).
 - [20] A. M. Reynolds, *Physica A* **388**, 561 (2009).
 - [21] K. Schwarz, Y. Schröder, B. Qu, M. Hoth, and H. Rieger, *Phys. Rev. Lett.* **117**, 068101 (2016).
 - [22] Z. Schuss, A. Singer, and D. Holcman, *Proc. Nat. Acad. Sci. U.S.A.* **104**, 16098 (2007).
 - [23] O. Bénichou and R. Voituriez, *Phys. Rev. Lett.* **100**, 168105 (2008).
 - [24] M. Mangeat and H. Rieger, *J. Phys. A* **52**, 424002 (2019).
 - [25] J. Noetel, V. Freitas, E. Macau, and L. Schimansky-

- Geier, Phys. Rev. E **98**, 022128 (2018).
- [26] J. Noetel, V. Freitas, E. Macau, and L. Schimansky-Geier, Chaos **28**, 106302 (2018).
- [27] G. Viswanathan, S. Buldyrev, S. Havlin, M. Da Luz, E. Raposo, and E. Stanley, Nature **401**, 911 (1999).
- [28] F. Bartumeus, J. Catalan, U. L. Fulco, M. L. Lyra, and G. M. Viswanathan, Phys. Rev. Lett. **88**, 097901 (2002).
- [29] V. Tejedor, R. Voituriez, and O. Bénichou, Phys. Rev. Lett. **108**, 088103 (2012).
- [30] H. D. Vuijk, A. Sharma, D. Mondal, J.-U. Sommer, and H. Merlitz, Phys. Rev. E **97**, 042612 (2018).
- [31] F. Peng, Y. Tu, J. C. Van Hest, and D. A. Wilson, Angew. Chem. Int. Ed. **54**, 11662 (2015).
- [32] L. Zhang, J. J. Abbott, L. Dong, K. E. Peyer, B. E. Kratochvil, H. Zhang, C. Bergeles, and B. J. Nelson, Nano Lett. **9**, 3663 (2009).
- [33] A. Einstein, Ann. Phys. (Berl.) **324**, 371 (1906).
- [34] H. C. Berg and D. A. Brown, Nature **239**, 500 (1972).
- [35] R. Ma, G. S. Klindt, I. H. Riedel-Kruse, F. Jülicher, and B. M. Friedrich, Phys. Rev. Lett. **113**, 048101 (2014).
- [36] P. Romanczuk, M. Bär, W. Ebeling, B. Lindner, and L. Schimansky-Geier, Eur. Phys. J. Spec. Top. **202**, 1 (2012).
- [37] C. Bechinger, R. Di Leonardo, H. Löwen, C. Reichhardt, G. Volpe, and G. Volpe, Rev. Mod. Phys. **88**, 045006 (2016).
- [38] J. Gillis, Math. Proc. Cambridge Phil. Soc. **51**, 639 (1955).
- [39] J. Masoliver, K. Lindenberg, and G. H. Weiss, Physica A **157**, 891 (1989).
- [40] B. M. Friedrich, Phys. Biol. **5**, 026007 (2008).
- [41] G. Reddy, A. Celani, and M. Vergassola, J. Stat. Phys. **163**, 1454 (2016).
- [42] H. E. Daniels, Proc. Roy. Soc. Edinb. A **63**, 290–311 (1952).
- [43] B. M. Friedrich and F. Jülicher, Proc. Natl. Acad. Sci. U.S.A. **104**, 13256 (2007).
- [44] B. M. Friedrich and F. Jülicher, Phys. Rev. Lett. **103**, 068102 (2009).
- [45] S. Blanco and R. Fournier, EPL **61**, 168 (2003).
- [46] O. Bénichou, M. Coppey, M. Moreau, P. Suet, and R. Voituriez, EPL **70**, 42 (2005).
- [47] L. Rothschild and M. M. Swann, J. Exp. Biol. **26**, 164 (1949).
- [48] E. L. Charnov, Theoret. Popul. Biol. **9**, 129 (1976).
- [49] W. Feller, *An introduction to probability theory and its applications*, vol. 2 (John Wiley & Sons, 2008).
- [50] H. C. Berg, *Random Walks in Biology* (Princeton University Press, 1993).
- [51] H. D. Vuijk, H. Merlitz, M. Lang, A. Sharma, and J.-U. Sommer, arXiv preprint arXiv:2009.09060 (2020).
- [52] H. C. Berg and E. M. Purcell, Biophys. J. **20**, 193 (1977).
- [53] W. Bialek and S. Setayeshgar, Proc. Nat. Acad. Sci. U.S.A. **102**, 10040 (2005).
- [54] T. Mora and I. Nemenman, Phys. Rev. Lett. **123**, 198101 (2019).
- [55] M. Novak and B. M. Friedrich, New J. Phys. (in press).
- [56] S. Lange and B. M. Friedrich, PLoS Comp. Biol. (arXiv:1912.09112) (in press).
- [57] A. Dvoretzky and P. Erdős, in *Proc. 2nd Berkeley Symp.* (1951), pp. 353–367.

Supplemental Material

Justus A. Kromer, Andrea Auconi, Benjamin M. Friedrich: **Composite search of active particles in three-dimensional space based on non-directional cues**

Numerical methods

For numeric integration of Eqs. (1), (2) for the inner search problem, we used an explicit Euler-Maruyama method with integration time step $\Delta t = 2 \times 10^{-3} R_0/v$. ABPs were initially positioned at R_1 with initial direction angle ψ distributed according to $p(\psi, t=0) = \sin(2\psi)$ for $\psi \in [0, \pi/2]$ [5]. Simulations were stopped after a maximum search time of $2 \times 10^4 R_0/v$ (corresponding to a maximum trajectory length of $10^3 R_1$). Consistent results were obtained in preliminary simulations of ABP trajectories in three-dimensional space using an Euler-Heun scheme with matrix exponentials for propagation of the Frenet-Serret frame.

To compute the effective probability distribution $\bar{p}_{\text{in}}(\bar{\tau}) = \int_0^\infty d\tau p_{\text{in}}(\tau) q_{\bar{\tau}}(\tau)$ for search agents with stochastic timer [blue curves in Fig. 2], we used simulation results for $p_{\text{in}}(\tau)$ for $0 \leq \tau \leq t_{\text{max}}$ with $t_{\text{max}} = 5 \times 10^4 \tau_0$, and extrapolated $\mathcal{F}(\tau) = c\tau^{-3/2}$ for $\tau > t_{\text{max}}$ with prefactor c determined by a fit.

Analytic derivation of scaling law

We can mathematically prove the observed power law scaling of the optimal inner search time τ_{opt} in the limit of low directional persistence, $D_{\text{rot}} \gg v/R_0$. In this limit, we can approximate the motion of the agent for inner search by diffusive motion with effective translational diffusion coefficient $D_{\text{eff}} = l_p v/3 = (2/3)vR_0$ (corresponding to the example of an effective translational diffusion coefficient of an ABP with rotational diffusion coefficient $D_{\text{rot}} = v/(4R_0)$ and persistence length $l_p = v/(2D_{\text{rot}}) = 2R_0$ as used in Fig. 2). For diffusive motion, the probability to find a spherical target of radius R_0 within time τ if starting at $R = R_1$, is given by

$$p_{\text{in}}(\tau) = \frac{R_0}{R_1} \left[1 - \text{Erf} \left(\frac{R_1 - R_0}{\sqrt{4D_{\text{eff}}\tau}} \right) \right] . \quad (\text{S1})$$

We include the derivation of Eq. (S1) for completeness: we consider the diffusion equation in spherical coordinates for a radially symmetric probability density $p(R, t)$ for position in three-dimensional space (with units of an inverse volume)

$$\frac{\partial}{\partial t} p = D_{\text{eff}} R^{-1} \frac{\partial^2}{\partial R^2} (Rp) \quad , \quad (\text{S2})$$

with initial condition $p(R, 0) = (4\pi R_1^2)^{-1} \delta(R - R_1)$, and absorbing boundary conditions at $R = R_0$, $p(R_0, t) = 0$, and use the method of images to find the time-dependent solution

$$p(R, t) = \frac{1}{4\pi R_1^2 \sqrt{4\pi D_{\text{eff}} t}} \frac{R_1}{R} \left[\exp \left(-\frac{(R - R_1)^2}{4D_{\text{eff}} t} \right) - \exp \left(-\frac{(R + R_1 - 2R_0)^2}{4D_{\text{eff}} t} \right) \right] .$$

This solution satisfies the absorbing boundary condition $p(R_0, t) = 0$ at $R = R_0$. Now, $p_{\text{in}}(\tau) = \int_0^\tau dt \mathcal{F}(t)$, where the probability current $J(t)$ at time t to the absorbing sphere of radius R_0 at the origin is given by $\mathcal{F}(t) = 4\pi R_0^2 D_{\text{eff}} \partial p(R, t) / \partial R|_{R=R_0}$.

Eq. (S1) becomes exact in the limit $l_p \ll R_0$. Note that a similar result, yet with additional prefactor $R_0 v / (4D_{\text{eff}})$, was derived for a case of intermediate persistence length l_p with $R_0 \ll l_p \ll R_1$ (or $R_0 v \ll D_{\text{eff}} \ll R_1 v$) [40]

$$p_{\text{in}}(\tau) = \frac{R_0 v}{4D_{\text{eff}}} \frac{R_0}{R_1} \left[1 - \text{Erf} \left(\frac{R_1}{\sqrt{4D_{\text{eff}}\tau}} \right) \right] . \quad (\text{S3})$$

Here, $D_{\text{eff}} = l_p v/3$ denotes the effective translational diffusion coefficient of a persistent random walk in three-dimensional space with general persistence length l_p .

For the rate k_{out} at which the ABP enters the target zone around some target, we have

$$k_{\text{out}} = \rho v \pi R_1^2 (1 - k_{\text{out}} \tau) = \frac{\rho v \pi R_1^2}{1 + \rho v \pi R_1^2 \tau} . \quad (\text{S4})$$

By combining Eq. (S1) and Eq. (S4), we obtain for the rate k of target encounter

$$k = k_{\text{out}} p_{\text{in}} = \frac{\rho v \pi R_0 R_1}{1 + \rho v \pi R_1^2 \tau} \left[1 - \text{Erf} \left(\frac{R_1 - R_0}{\sqrt{4D_{\text{eff}}\tau}} \right) \right] . \quad (\text{S5})$$

In the limit of small targets $R_0 \ll R_1$, we can rewrite this expression as

$$k = \rho \pi R_0 R_1 v \frac{\beta^2}{\beta^2 + \Lambda} [1 - \text{Erf}(\beta)] \quad , \quad (\text{S6})$$

where we introduced short-hand

$$\Lambda = \frac{3\pi}{8} \frac{R_1}{R_0} \rho R_1^3, \quad \beta^2 = \frac{3}{8} \frac{R_1}{v\tau} \frac{R_1}{R_0} = \frac{R_1^2}{4D_{\text{eff}}\tau} . \quad (\text{S7})$$

In the limit $\Lambda \ll 1$, corresponding to $\rho V_1 \ll R_0/R_1$, we find that k becomes maximal for $\beta_{\text{opt}} = \pi^{1/6} \Lambda^{1/3}$. Thus, the optimal inner search time τ_{opt} reads

$$\tau_{\text{opt}} = \frac{3^{1/3}}{2\pi} \frac{R_0}{v} (\rho R_0^2 R_1)^{-2/3} . \quad (\text{S8})$$

Hence, τ_{opt} decreases if R_0 or R_1 become larger, and increases if targets become sparser.

In the limit $\rho V_1 \ll R_0/R_1$ with $\beta \ll 1$, the success probability of inner search approaches the limit value for time-unrestricted diffusive search, $\lim_{\tau \rightarrow \infty} p_{\text{in}} = R_0/R_1$. The time fraction spent in inner search mode is negligible in this limit, $k\tau \approx (R_0^2 R_1 \rho)^{1/3} \ll 1$. For the rate k of target encounter, we find

$$k \approx \rho \pi R_0 R_1 v \quad . \quad (\text{S9})$$

This result corresponds to an effective cross-sectional area of the target $k/(v\rho) \approx \pi R_0 R_1$ for the case of composite search with fixed inner search considered here (in the appropriate limit case), see also Table S1.

Reference case: Global diffusive search

As a reference case, we additionally consider a case of effective diffusive search without time-restriction, and a high rotational diffusion coefficient $D_{\text{rot}} \gg v/R_0$ that is constant in time and space. As always, we consider search in three-dimensional space for randomly distributed non-revisitable targets. A calculation analogous to the derivation of Eq. (S9) yields the steady-state target encounter rate k_{diff} for this case (time-unrestricted diffusive search for non-revisitable targets in three-dimensional space). This rate is well defined only in dimension $d \geq 3$, which follows from Pólya's classical result on time-discrete random walks on a d -dimensional lattices [57].

We first consider a purely diffusive search agent with effective translational diffusion coefficient D_{eff} in three-dimensional space, as well as Poisson distributed spherical targets with radii R_0 . We switch to a coordinate frame that is co-moving with the diffusive agent. In this frame, the centers of the targets are diffusing and become absorbed once they reach a spherical shell of radius R_0 concentric with the agent. We make the simplifying assumption that the diffusive motion of the target centers can be considered independent. The probability density $p_{\text{target}}(R, t)$ of those target centers that have not yet been absorbed is radially symmetric (with units of an inverse volume) and obeys the diffusion equation Eq. (S2). The steady-state probability density reads

$$p_{\text{target}}^*(R) = \rho \left(1 - \frac{R_0}{R} \right) \quad , \quad (\text{S10})$$

satisfying the boundary conditions $p_{\text{target}}^*(R_0) = 0$ and $\lim_{R \rightarrow \infty} p_{\text{target}}^*(R) = \rho$. Thus, we find for the steady-state current of target centers to the absorbing shell

$$k_{\text{diff}} = 4\pi R_0^2 D_{\text{eff}} \frac{\partial}{\partial R} p_{\text{target}}^*(R)|_{R=R_0} \quad (\text{S11})$$

$$= \rho 4\pi R_0 D_{\text{eff}} \quad . \quad (\text{S12})$$

An ABP with high rotational diffusion coefficient $D_{\text{rot}} \gg v/R_0$ can be approximately described as a diffusive particle with effective translational diffusion coefficient $D_{\text{eff}} = l_p v/3$, where $l_p = v/(2D_{\text{rot}})$ denotes the persistence length of the ABP. Thus,

$$\frac{k_{\text{diff}}}{\rho v} \approx \frac{4\pi}{3} R_0 l_p \quad . \quad (\text{S13})$$

Limit values of target encounter rate

We report limit values of the target encounter rate k for different inner search strategies in the limit of large rotational diffusion coefficients, see table S1. Target encounter rates are reported as an effective cross-sectional area of the targets, $k/(v\rho)$. For the case of fixed inner search time with effective diffusive motion in inner search (first column), the target encounter rate equals $k = k_{\text{out}} p_{\text{in}}$, where $k_{\text{out}}/(v\rho) = \pi R_1^2$ is the normalized rate of target encounter for ballistic outer search, and $p_{\text{in}} \approx R_0/R_1$ the success probability of inner search. For the case of adaptive inner search [with ballistic motion for $R \leq R_1$ and effective diffusive motion for $R > R_1$, strategy (ii)] (second column), inward scattering of outgoing trajectories implies $p_{\text{in}} \lesssim 1$ [5]. For comparison, we also report the case of purely ballistic search, where the ABP employs $D_{\text{rot}} = 0$ both for outer and inner search (third column); in this case, $k/(v\rho) = \pi R_0^2$. Finally, we consider a case of inverted adaptive search, where the ABP employs a high rotational diffusion coefficient $D_{\text{rot}} = D_1 \gg v/R_0$ inside the target zone defined by $R \leq R_1$, but ballistic motion outside, $D_{\text{rot}} = D_2 = 0$ (fourth column). In this case, $p_{\text{in}} \approx 0$ as consequence of an outward scattering effect of ingoing trajectories [5].

Lastly, one may ask about composite search strategies that employ effective diffusive motion in outer search, with high rotational diffusion coefficient D_{rot} . In this case, a composite search with constant rotational diffusion coefficient during inner search (e.g., *fixed inner search time*) does not provide any considerable benefit. Only adaptive inner search considerably increases the rate of target encounter, yielding $k/(v\rho) \approx (4\pi/3) R_1 l_p$, where $D_2 = v/(2l_p) \gg v/R_0$ is the rotational diffusion coefficient used during inner search outside the target zone. (Here, we used Eq. (S13) for k_{out} , replacing R_0 by R_1 , and $p_{\text{in}} \approx 1$.) However, this rate is still smaller than the corresponding rate for adaptive inner search and ballistic outer search, see Table S1.

Strategy for <i>inner search</i> (<i>outer search</i> : ballistic)			
Fixed inner search time	Adaptive inner search	Ballistic inner search	Inverted adaptive inner search
$\pi R_0 R_1$	πR_1^2	πR_0^2	0

TABLE S1: Normalized rate of target encounter for different inner search strategies reported as $k/(v\rho)$ with units of an effective cross-sectional area of targets. We assume ballistic motion with $D_{\text{rot}} = 0$ in outer search throughout. **First column:** we consider diffusive motion with constant rotational diffusion coefficient $D_{\text{rot}} \gg v/R_0$, corresponding to the strategy (i-a) of *fixed inner search time* considered in the main text. Analogous results are found for the strategy (i-b) with *stochastic timer* with random inner search times. **Second column:** we consider *adaptive inner search*, strategy (ii), with position-dependent rotational diffusion coefficient $D_{\text{rot}}(\mathbf{x})$ ($D_1 = 0$ and $D_2 \gg v/R_0$) as considered in the main text. **Third column:** additionally, we state the result for an ABP that moves always ballistically, i.e., for which outer and inner search are indistinguishable. **Fourth column:** finally, we consider an inverted adaptive inner search strategy, where the position-dependent rotational diffusion coefficient $D_{\text{rot}}(\mathbf{x})$ equals $D_1 \gg v/R_0$ for $R \leq R_1$ and $D_2 = 0$ for $R > R_1$.